RSC Advances

PAPER

View Article Online
View Journal | View Issue

Cite this: *RSC Adv.*, 2020, **10**, 14953

Colorimetric determination of ascorbic acid based on carbon quantum dots as peroxidase mimetic enzyme

Xin Shu,[a] Yuwai Chang,[a] Huizhong Wen,[a] Xiaotiao Yao[a] and Yilin Wang *[ab]

Carbon quantum dots (CQDs) were synthesized from litchi peel, exhibiting a peroxidase-like activity and enabling the oxidation of 3,3′,5,5′-tetramethylbenzidine (TMB) in association with H_2O_2 to generate blue oxidized TMB (ox-TMB) with a strong absorption peak at 652 nm. Interestingly, the ox-TMB could be further reduced by ascorbic acid (AA) leading to fading of the blue color and an absorbance decrease. Thus, a convenient and sensitive colorimetric method for detection of AA using CQDs as peroxidase mimics was established. Several factors, such as acidity, temperature, incubating time, and TMB concentration, which might influence the response of the analysis signal, were optimized. The results showed that the decrease of absorbance (ΔA) was in good linear agreement with AA concentration in the range of 1.0–105 μM, with a low detection limit of 0.14 μM. The feasibility of this method was also investigated in commercial beverages with the 94.3–110.0% recovery.

Received 5th March 2020
Accepted 1st April 2020

DOI: 10.1039/d0ra02105a

rsc.li/rsc-advances

1 Introduction

Ascorbic acid (AA), which plays vital roles in biological reactions such as free radical scavenging, cancer inhibition and prevention, is commonly found in food, plant and animal tissues.[1] Due to its excellent antioxidant property, AA is one of the most significant vitamins and can induce protection against oxidative stress.[2,3] Medical research has revealed that AA can be used to treat colds, mental disorders, infertility, cancer, and AIDS. Thus, for the sake of monitoring its content and to provide guidance for medical diagnosis and diet, the development of a reliable, selective and simple method for AA determination has become vital. Some traditional methods including iodimetric titration, electrochemistry,[4] high performance liquid chromatography,[5] fluorescence,[6] capillary electrophoresis[7] and enzyme-linked immunosorbent assay (ELISA)[8] have been proposed for detection of AA. Despite the successful detection results, iodimetric titration is only suitable for macro-analysis, and most of the other methods suffer from the obstacles such as requirement for sophisticated equipment, skilled technicians, complicated sample pretreatment, or high-cost biological reagents. Due to the advantages of fast response, simple operation and high sensitivity, colorimetrical method has been preferred.[9]

In recent years, artificial enzymes based on nanomaterials have become a research preference. [10] Varied types of nanomaterials, such as metal oxides,[11–13] metal sulfides,[14,15] noble metal[16] and carbon quantum dots (CQDs),[17–19] have been reported to exhibit unique properties of peroxidase mimic and successfully applied in many fields. Among these, CQDs are paid extensively attention due to their ease synthetic methodology, superior optical properties, low toxicity and good biocompatibility.[20–24] Since Shi and coworkers reported that CQDs could act as peroxidase mimics, CQDs have achieved a rapid development and many applications in a new field.[25] In this work, CQDs was synthesized from a discarded natural biomass – litchi peel, which could catalyze the oxidation of colorless 3,3′,5,5′-tetramethylbenzidine (TMB) in association with H_2O_2 to generate a blue product (ox-TMB).[26,27] The introduction of AA would result in the reduction of ox-TMB to native TMB, leading to the blue color fading (Scheme 1). On this basis, a colorimetric method for AA detection was developed using the catalytic active CQDs and good sensitivity and selectivity in commercial beverage sample analysis were achieved.

Litchi peel is a commonly discarded natural biomass in south China. In comparison with the reported CQDs with peroxidase-like catalytic activities, the present CQDs synthesized with litchi peel that can be obtained with low cost, and adequate supply source, indicating that the method is suitable for large-scale preparation of catalytically active CQDs.

2 Experimental

2.1 Materials and method

All the reagents were of analytical grade and used as received. Double deionized water (DDW) was used for aqueous solutions. AA and TMB were obtained from Aladdin Reagent Company

[a]School of Chemistry and Chemical Engineering, Guangxi University, Guangxi Key Laboratory of Biorefinery, Nanning 530004, China
[b]Guangxi Key Laboratory of Biorefinery, Nanning 530004, China. E-mail: theanalyst@163.com; Tel: +86 771 3392879

(Shanghai, China). Sodium acetate (NaAc), Acetic acid (HAc), *N*,*N*-dimethylformamide (DMF), tartaric acid (TA) and benzoic acid (BA) were acquired from Guangdong Guanghua Sci-Tech Co., Ltd. Three kinds of Vitamin (VB1, VB2, VB6) were purchased from Sinopharm Chemical Reagent Co., Ltd. Glycine (Gly), threonine (Thr), phenylalanine (Phe), lysine (Lys), histidine (His), alanine (Ala), glucose (Glu), lactose (Lac) and fructose (Fru) were procured from Da Mao Chemical Reagents (Tianjin, China).

UV-vis spectra were recorded on a UV-4802 spectrophotometer (Unico, Shanghai, China). High-resolution transmission electron microscopy (HRTEM) image was obtained with 200 kV accelerating voltage (Tecnai G2 F20 S-TWIN, FEI Company, USA). FTIR spectra were taken at Nicolet iS50 spectrometer (Thermo Scientific Co., Ltd. Madison, WI, USA).

2.2 Synthesis of CQDs

The water-soluble CQDs originated from litchi peel were synthesized as reported in our previous work.[28] Litchi peel was dried at 60 °C to constant weight after washed by water. Next, the dried peel was put into a crucible and carbonized on an electric furnace. After ground, it was cleaned with acetone and then dried at 110 °C. Mixed 0.5 g of carbonized peel with 150 mL of 5 M HNO_3 and refluxed for 12 h at 140 °C. The supernatant was neutralized with sodium carbonate and dialyzed with DDW (cut off molecular weight 8000–14 000) for 24 h. Then acetone was poured into the purified solution and centrifuged for 15 min at 16 000 rpm. The solid was collected and dried at 40 °C in vacuum oven. After dissolved in DDW, the large particles were removed by ultra-filtration with 0.22 μm ultrafiltration membrane. Finally, a brown CQDs solution with high purity and good clarity was achieved and stored at 4 °C for further use.

2.3 Procedure for determination of AA

In a series 10 mL colorimetric tubes, 0.5 mL of 500 μg mL^{-1} CQDs, 1.0 mL of 20 mM TMB, 1.0 mL of 40 mM H_2O_2, 7.2 mL of NaAc-HAc buffer (pH 3.5) and 300 μL of AA standard at different concentration were added sequentially. Then, the above-prepared solutions were shaken and incubated at 35 °C for 20 min prior to UV-vis detection at 652 nm. Three parallel measurements were performed.

2.4 Determination of AA in real samples

Two kind of popular tea beverages (Oolong tea and Oriental Leaf Black tea) were obtained from a local supermarket. First, dilute the beverage sample by 2 times. The 1.00 mL diluted solution was then mixed with the above CQDs–H_2O_2–TMB system. The content of AA was calculated against the standard calibration curve of UV-vis detection.

3 Results and discussion

3.1 Characterization of CQDs

The statistical result displays that most of the CQDs' diameter are in the range of 2.1–4.5 nm with the average diameter of 3.1 nm (Fig. 1A, inset), demonstrating an excellent uniform particle size distribution. The peaks at 1396 cm^{-1} and 3367 cm^{-1} in FTIR (Fig. 1C) are ascribed to the in-plane bending vibration and stretching vibration of –OH, respectively. The peaks at 1608 cm^{-1} and 1130 cm^{-1} are attributed to the stretching vibrations of C=O and C–O, individually. These characteristic peaks suggest that the CQDs have good water solubility and are consistent with the report.[29] XRD pattern (Fig. 1D) presents a diffraction peak at $2\theta = 25°$, indicating the planes of graphite lattice spacing (002). All information confirms the existence of CQDs.

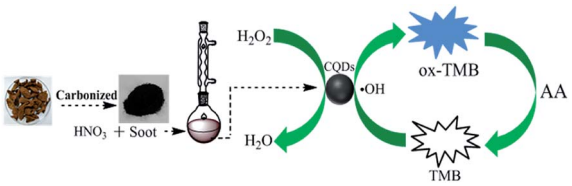

Scheme 1 Sketch of the preparation of CQDs from litchi peel and the detection mechanism for AA.

3.2 The catalysis and detection mechanism

The possible mechanism of peroxidase-like mimetic activity of CQDs was proposed in previous reports.[25,30] It confirmed that during the oxidation process of TMB, ˙OH radical was formed by the reduction of H_2O_2 that facilitated the electron transfer from ˙OH radical to TMB, and CQDs played a vital role to produced ˙OH radical. In addition to this, at the negatively charged CQDs, the positively charged TMB accumulated and enhanced the electronic charge on CQDs which facilitated the reduction of H_2O_2 to produced ˙OH radical. Hence, the ˙OH radical was undergoing one electron transfer to ease the oxidation of TMB.

The absorption spectra of different systems are showed in Fig. 2. At 652 nm only a weak absorption peak appears in the TMB + H_2O_2 system, while it becomes strong and significant in the CQDs + H_2O_2 + TMB system (curve d and curve a, respectively). Meanwhile, the solution transforms from almost colorless to dark blue (first right and first left of illustration,

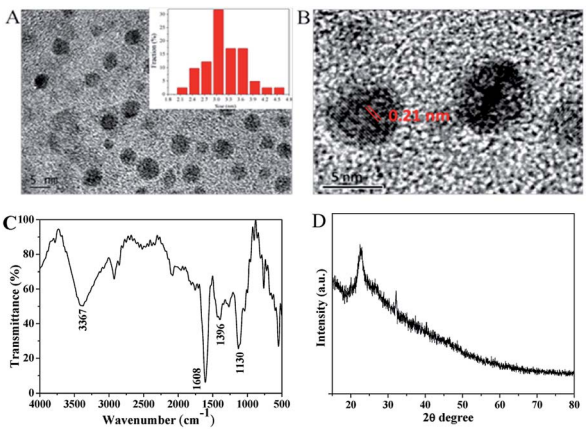

Fig. 1 (A) TEM image of the CQDs, (B) HRTEM image of the CQDs, (C) FTIR spectra of the CQDs, (D) XRD pattern of the CQDs.

respectively). This demonstrates that the CQDs catalyze the oxidation of colorless TMB in association with H_2O_2 to generate a blue product of ox-TMB (eqn 1). The addition of AA to the CQDs–H_2O_2–TMB system can reduce the absorbance. A low AA concentration of 20 μM gives rise to minor changes in absorbance and color (curve b, second left of illustration). However, a high AA concentration of 60 μM results in a sharp decrease in absorbance and significant fading (curve c, second right of illustration). The experiment confirms that AA is able to reduce ox-TMB (eqn 2),[30] translating into the decrease of absorbance. The decreased value is related to the concentration of AA. Thus, the CQDs + H_2O_2 + TMB system provides a rapid and sensitive colorimetric approach to detect AA.

$$H_2O_2 + TMB \xrightarrow{CQDs} H_2O + \text{ox-TMB} \quad (1)$$

$$AA + \text{ox-TMB} \rightarrow DHAA + TMB + H^+ \quad (2)$$

3.3 Optimization of detection conditions

The peroxidase activity of CQDs was affected by pH value, incubation temperature, incubation time and TMB concentration. Therefore, the experimental conditions of the above parameters were optimized before application. Δ*A* represents the absorbance reduction at 652 nm caused by AA.

The pH value is an important factor in the determination. It can be seen from Fig. 3A that Δ*A* increases with the increase of pH value between 2.5 and 3.5, but decreases with the further increase of pH value from 3.5 to 5.5. Δ*A* peak appears at pH 3.5, which is consistent with the previous report,[31,32] so it is adopted. As shown in Fig. 3B, the influence of incubation temperature on Δ*A* was studied. Δ*A* reached its maximum when the temperature is 35 °C. With the further increase of temperature from 35 °C to 45 °C, Δ*A* decreases. Accordingly, 35 °C is chosen for further experiments. Various incubation time intervals from 5 to 30 min are investigated and the maximum of Δ*A* is showed at 20 min (Fig. 3C). Fig. 3D displays the effect of TMB concentration on Δ*A*. Results show that too high or too low TMB concentration is not suitable for AA determination. When TMB concentration is 2.0 mM, Δ*A* reaches the maximum value.

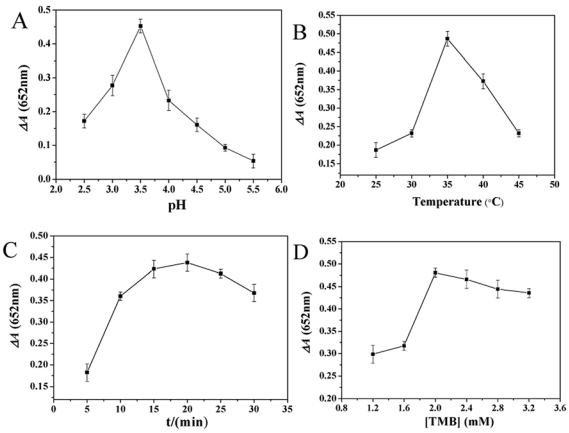

Fig. 3 Optimization of AA detection conditions. The effects of (A) pH, (B) incubation temperature, (C) incubation time, (D) TMB concentration on Δ*A*.

Consequently, the prepared CQDs exhibit the strongest catalytic activity at pH 3.5, incubation temperature of 35 °C, incubation time of 20 min and TMB concentration of 2.0 mM.

3.4 Analysis performance

AA was detected under the optimized condition. The UV-vis absorption spectra of different AA concentration systems are shown in Fig. 4A. Obviously, the absorbance of 652 nm decreased with the increase of AA concentration. In the range of 1.0–105 μM, there is a good linear relationship between Δ*A* and AA concentration with a regression equation of $\Delta A = 0.0075C + 0.023$ ($R^2 = 0.999$) (Fig. 4B). According to the 3σ/slope law, the limit of detection (LOD) reached 0.14 μM. After comparing the present detection method to the already reported detection system, it was found that the proposed method exhibited lower LOD with excellent linearity range than most reports (Table 1).

To investigate the selectivity of the proposed method, the effects of some interfering substances were investigated, including BA, TA, VB_1, VB_2, VB_6, Glu, Fru, Lac, Gly, Thr, His, Lys, Ala, Phe and 5 kinds of cations (Cu^{2+}, Zn^{2+}, Ca^{2+}, K^+ and Mg^{2+}). Results in Fig. 5 show that only AA yields a significant change in absorbance; whereas the change observed in the presence of other potential interference is negligible, suggesting that the proposed assay possesses a high selectivity toward AA.

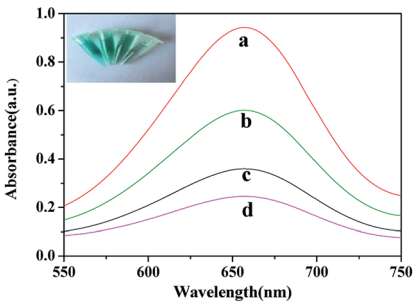

Fig. 2 Absorption spectra of (a) CQDs + TMB + H_2O_2; (b) CQDs + TMB + 20 μM (AA) + H_2O_2; (c) CQDs + TMB + 60 μM (AA) + H_2O_2; (d) TMB + H_2O_2. The corresponding photo images are shows in the illustration.

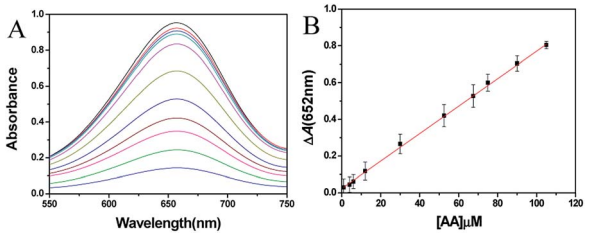

Fig. 4 (A) Absorption spectra of CQDs + TMB + H_2O_2 system upon adding various concentrations of AA (from top to bottom: 0.00, 1.0, 4.0, 6.0, 12.0, 30.0, 52.5, 67.5, 75.0, 90.0, 105 μM). (B) The linear relationship between Δ*A* and AA concentration.

Table 1 Comparison of different AA analysis methods

Method	System	Response time	Linear range (μM)	LOD (μM)	Ref.
Fluorimetry	GQDs	70 min	0.05–6	0.021	33
Fluorimetry	CQDs/AuNCs	No report	0.15–15	0.105	34
Electroche-mical	3D-rGO/Fe_3O_4/HP-β-CD/GCE	No report	15–360	5	35
Colorimetry	Pd/PPy	210 s	2–40	0.062	36
Colorimetry	PSS-rGO	No report	0.8–60	0.15	37
Colorimetry	Cu–Ag/rGO	50 min	5–30	3.6	38
Colorimetry	Mn-CDs	No report	0.05–2.5	0.009	39
Colorimetry	Co_3O_4/CGM	10 min	30–140	0.19	40
Colorimetry	M-CQDs	40 min	10–75	3.26	30
Colorimetry	ClO^-/TMB	30 s	1–70	0.58	41
Colorimetry	Ag^+–TMB	5 min	0.5–60	0.23	31
Colorimetry	CQDs	20 min, 25 min	1.0–105	0.14	This work

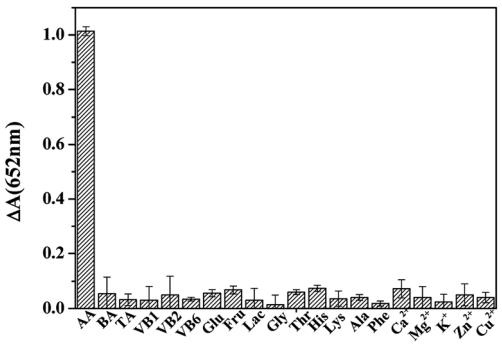

Fig. 5 Selectivity of AA detection. Concentration: AA: 45 μM; interference: 45 μM.

Furthermore, the intrinsic color of tea beverages is not blue, and there is no absorbance at the measured wavelength. Thus, this method does not require complex sample treatment and is suitable for AA sensing in beverage sample.

3.5 AA detection in real samples

AA detection was carried out on real samples for the practicability validation. The content of AA in commercial beverages was detected using standard addition method. The concentration of AA in two dilution samples was determined as 49.0 μM and 39.0 μM, respectively. Taken the 20-fold dilution into calculation, AA concentrations of the two beverage samples are 172.6 mg L^{-1} and 137.4 mg L^{-1}, respectively, which agree well with those claimed. Furthermore, Table 2 shows that the recovery is ranging from 94.3% to 110.0%, while RSD is between 0.4% and 3.5%. These indicate the CQDs-based peroxidase-like detection system is characterized by high accuracy, precision and practicability for application.

Table 2 Recoveries experiments results of AA in real samples

Samples	Spiked (μM)	Found (μM)	Recovery (%)	RSD (%)
Oolong tea beverage	0.00	49.0	—	1.7
	10.0	60.0	110.0	1.5
	20.0	68.0	95.0	3.5
Black tea beverage	0.00	39.0	—	0.4
	10.0	49.3	103.0	0.9
	20.0	57.8	94.3	2.2

4 Conclusions

In summary, peroxidase-like activity CQDs, synthesized from litchi peel, could be used to catalyze the oxidation of TMB in association with H_2O_2 to generate blue ox-TMB. The ox-TMB could be further reduced by AA leading to a blue fading and an absorbance decrease. Based on this, we established a convenient and sensitive colorimetric method for AA assay using CQDs as peroxidase mimics. The LOD of AA detection was found to be 0.14 μM. The practicability was investigated in commercial beverages with the recovery between 94.3%–110.0%. Compared with natural enzymes, CQDs as peroxidase mimetic have the advantages of easy preparation, high stability, cost effective and resistant inactivation.

Conflicts of interest

There are no conflicts to declare.

Acknowledgements

This work was financially supported by the Natural Science Foundation of Guangxi (2018GXNSFAA050015), the Dean Project of Guangxi Key Laboratory of Biorefinery (GXKLB-201801) and the Foundation of College Student Innovation Ability Training of Guangxi University (201910593184).

References

1 P. Kalimuthu and S. John, *Bioelectrochemistry*, 2009, **77**, 13–18.

2 S. Padayatty, A. Katz, Y. Wang, P. Eck, O. Kwon, J. Lee, S. Chen, C. Corpe, A. Dutta, S. Dutta and M. Levine, *J. Am. Coll. Nutr.*, 2003, **22**, 18–35.
3 M. Gao, X. Lu, G. Nie, M. Chi and C. Wang, *Nanotechnology*, 2017, **28**, 485708.
4 M. Sajid, S. Khan, N. Shad, N. Amin and Z. Zhang, *RSC Adv.*, 2018, **8**, 23489–23498.
5 P. Jiang, G. Huang, L. Jmaiff Blackstock, J. Zhang and X. Li, *Anal. Chem.*, 2017, **89**, 13642–13650.
6 L. Hu, L. Deng, S. Alsaiari, D. Zhang and N. Khashab, *Anal. Chem.*, 2014, **86**, 4989–4994.
7 W. Kim, R. Dahlgren, L. Moroz and J. Sweedler, *Anal. Chem.*, 2002, **74**, 5614–5620.
8 S. Uchiyama, Y. Kobayashi, S. Suzuki and O. Hamamoto, *Anal. Chem.*, 1991, **63**, 2259–2262.
9 S. Chandra, V. Singh, P. Yadav, D. Bano, V. Kumar, V. Pandey, M. Talat and S. Hasan, *Anal. Chim. Acta*, 2019, **1054**, 145–156.
10 M. Ashrafizadeh, R. Mohammadinejad, S. Kailasa, Z. Ahmadi, E. Afshar and A. Pardakhty, *Adv. Colloid Interface Sci.*, 2020, **278**, 102123.
11 Y. Ma, Z. Zhang, C. Ren, G. Liu and X. Chen, *Anal*, 2012, **137**, 485–489.
12 H. Zhao, Y. Dong, P. Jiang, G. Wang and J. Zhang, *ACS Appl. Mater. Interfaces*, 2015, **7**, 6451–6461.
13 J. Mu, Y. Wang, M. Zhao and L. Zhang, *Chem. Commun.*, 2012, **48**, 2540–2542.
14 T. Lin, L. Zhong, Z. Song, L. Guo, H. Wu and Q. Guo, *Biosens. Bioelectron.*, 2014, **62**, 302–307.
15 X. Guo, Y. Wang, F. Wu, Y. Ni and S. Kokot, *Anal*, 2015, **140**, 1119–1126.
16 C. Lien, Y. Chen, H. Chang and C. Huang, *Nanoscale*, 2013, **5**, 8227–8234.
17 B. Wang, F. Liu, Y. Wu, Y. Chen, B. Weng and C. Li, *Sens. Actuators, B*, 2018, **255**, 2601–2607.
18 Q. Zhong, Y. Chen, A. Su and Y. Wang, *Sens. Actuators, B*, 2018, **273**, 1098–1102.
19 S. Kailasaa, S. Ha, S. Baek, L. Phan, S. Kim, K. Kwak and T. Park, *Mater. Sci. Eng., C*, 2019, **98**, 834–842.
20 M. Amjadia, T. Hallaja, H. Asadollahia, Z. Songb and M. Frutosc, *Sens. Actuators, B*, 2017, **244**, 425–432.
21 Y. Hu, L. Zhang, X. Geng, J. Ge, H. Liu and Z. Li, *Anal. Methods*, 2017, **9**, 5653–5658.
22 A. Su, D. Wang, X. Shu, Q. Zhong, Y. Chen, J. Liu and Y. Wang, *Chem. Res. Chin. Univ.*, 2018, **34**, 164–168.
23 V. Mehta, S. Jha and S. Kailasa, *Mater. Sci. Eng., C*, 2014, **38**, 20–27.
24 V. Mehta, S. Jha, H. Basu, R. Singhal and S. Kailasa, *Sens. Actuators, B*, 2015, **213**, 434–443.
25 W. Shi, Q. Wang, Y. Long, Z. Cheng, S. Chen, H. Zheng and Y. Huang, *Chem. Commun.*, 2011, **47**, 6695–6697.
26 W. Zhu, J. Zhang, Z. Jiang, W. Wang and X. Liu, *RSC Adv.*, 2014, **4**, 17387–17392.
27 B. Garg and T. Bisht, *Molecules*, 2016, **21**, 1653.
28 Q. Zhong, Y. Chen, X. Qin, Y. Wang, C. Yuan and Y. Xu, *Microchim. Acta*, 2019, **186**, 161.
29 Y. Song, K. Qu, C. Zhao, J. Ren and X. Qu, *Adv. Mater.*, 2010, **22**, 2206–2210.
30 S. Chandra, V. Singh, P. Yadav, D. Bano, V. Kumar, V. Pandey, M. Talat and S. Hasan, *Anal. Chim. Acta*, 2019, **1054**, 145–156.
31 X. Shu, Y. Chen, C. Yuan and Y. Wang, *New J. Chem.*, 2020, **44**, 1772–1776.
32 Y. Ding, B. Yang, H. Liu, Z. Liu, X. Zhang, X. Zheng and Q. Liu, *Sens. Actuators, B*, 2018, **259**, 775–783.
33 H. Liu, N. Lia, H. Zhang, F. Zhang and X. Su, *Talanta*, 2018, **189**, 190–195.
34 W. Niu, D. Shan, R. Zhu, S. Deng, S. Cosnier and X. Zhang, *Carbon*, 2016, **96**, 1034–1042.
35 W. Liang, Y. Rong, L. Fan, C. Zhang, W. Dong, J. Li, J. Niu, C. Yang, S. Shuang, C. Dong and W. Wong, *Microchim. Acta*, 2019, **186**, 751.
36 M. Zhong, M. Chi, Y. Zhu, C. Wang and X. Lu, *Anal. Chim. Acta*, 2019, **1056**, 125–134.
37 J. Chen, J. Ge, L. Zhang, Z. Li, J. Li, Y. Sun and L. Qu, *Microchim. Acta*, 2016, **183**, 1847–1853.
38 G. Darabdhara, B. Sharma, M. Das, R. Boukherroub and S. Szuneritsc, *Sens. Actuators, B*, 2017, **238**, 842–851.
39 S. Zhuo, J. Fang, M. Li, J. Wang, C. Zhu and J. Du, *Microchim. Acta*, 2019, **186**, 745.
40 S. Fan, M. Zhao, L. Ding, H. Li and S. Chen, *Biosens. Bioelectron.*, 2017, **89**, 846–852.
41 C. Mu, H. Lua, J. Bao and Q. Zhang, *Spectrochim. Acta, Part A*, 2018, **201**, 61–66.